# Stony Brook University

**Adsorption of polybutadiene from the melt onto solid substrates**

A Dissertation Presented

by

**Zexi Han**

to

The Graduate School

in Partial Fulfillment of the

Requirements

for the Degree of

**Master of Science**

in

**Materials Science and Engineering**

Stony Brook University

**May 2012**

**Stony Brook University**

The Graduate School

**Zexi Han**

We, the dissertation committee for the above candidate for the

Master of Science degree, hereby recommend

acceptance of this dissertation.

**Tadanori Koga --- Thesis Adviser Assistant Professor, Materials Science and Engineering**

**Jonathon Sokolov --- Second Reader Professor, Materials Science and Engineering**

**T.A Venkatesh---Third Reader Assistant Professor, Materials Science and Engineering**

This dissertation is accepted by the Graduate School

Charles Taber

Interim Dean of the Graduate School

Abstract of the Dissertation

**Adsorption of polybutadiene from the melt onto solid substrates**

by

**Zexi Han**

**Master of Science**

in

**Materials Science and Engineering**

Stony Brook University

**2012**

In this paper, adsorbed polybutadiene (PB) layers onto solid substrates have been studied with two different molecular weights and different terminated groups. Spin cast PB film (originally around 25 nm in thickness) prepared on two kinds of preconditioning (with and without HF etch) in silicon substrates. The samples were annealed at 150ºC for 10 h under vacuum and subsequently rinsed with toluene (a good solvent for PB) extensively. The residual PB layers were characterized by using X-ray reflectivity, and the result showed that the adsorbed layers were well fitted by a 3-layer (a silicon substrate, a native oxide, a polymer layer) model for non-end functionalized PB and a 4-layer model (a silicon substrate, a native oxide, a high density polymer layer and low density polymer layer) for hydroxyl PB adsorbed layer, respectively. Further experiments using supercritical carbon dioxide ($scCO_2$) as a screen solvent proved that the interfacial energy is a key to explain the difference in the structures between the two polybutadiene adsorbed layers.

## Table of Content

## List of figures

## List of tables

**Acknowledgement**

First I would like to express my sincere gratitude to Professor Tadanori Koga, my academic advisor, for his excellent guidance and constant support during these years. Without his instructions and ideas this thesis cannot be finished.

The support of my senior Peter Gin and Naisheng Jiang are greatly appreciated. I am very grateful for their support and constructive comments. They really helped me a lot for my research.

Many thanks to all the members from Koga's group. I learned a lot of useful experiences from my colleagues and seniors. I truly feel blessed to have such a wonderful group.

Special thanks to all my friends at Stony Brook University and people from Materials Science and Engineering department.

## Chapter 1 Introduction

Polymer thin films (thicknesses between 1000 and 10,000 angstroms) and ultra thin polymer films (thicknesses less than 1000 angstroms) are being used in many application such as resists, interlayer dielectrics in microelectronics fabrication, alignment layers in liquid crystal displays, and as lubricants in magnetic information storage devices [1]. Polymer chain orientation and state of organization play important roles in determining the final properties of these applications such as flow and intermolecular entanglements, local chain mobility and glass transition temperature (Tg), physical aging, creep behavior, gas permeability and crystallization kinetics can differ substantially from their bulk values. [1] [2] Polymer thin films are usually fabricated by using a spin-coating method, which is performed by dropping a small quantity of a polymer solution on a flat and clean substrate and then rotating the substrate at a given rotation speed for a given time. The films are typically annealed to remove residual solvent and to relax internal stresses. [3]

There has been a number of evidence over the past two decades showing that the deviations from bulk properties often when polymers are prepared as such thin films, especially when the film thickness is comparable to the gyration radius of the polymer (typically 2 to 50 nm). It is called as nanoconfinement effects and there report many unusual phenomena including crystallization, [3-6] physical cross-linking in associative polymers, [7] thermal expansion coefficients, [8-13] the glass transition temperature (Tg). [14]. In addition, many previous studies revealed that the structural [14-19] and dynamical properties [14, 19-25] in thin films could be different from those of the bulk [26].

Confinement effect can also influence conformation and intertwining of the polymer chains. Structural changes resulted by the interaction with a solid substrate would affect dynamical aspects as well as adhesion and wetting characteristic. [26,27] Theoretical studies and computer simulations [28-33] suggest that these static properties such as local density differ from bulk values only up to a few segmental layers away from an interface. [34]

Recently, great attention has been paid to absorbed polymer chains, which directly contact with a substrate surface composed of loops and tails [36]. Guiselin [37] discussed the adsorption mechanism of polymer melts in contact with a neutral wall using the random-walk model. He showed that, after removal of unbound material, the swelling of the residual bound layer in a good solvent shows a brush-like [38] behavior showing results with height $h_{swollen} \sim N_{5/6}$and segment density profile φ (z) $\sim z^{-2/5}$, where $z$ denotes the distance away from the substrate. [37] In Guiselin's thought, experiments are possible but difficult to achieve in practice. Generally, it has to equilibrate the melt or dense solution against the substrate surface, and make the polymer segment absorbed in a short time. All the experimental results concerned about a substrate surface, with a large barrier to segmental desorption always in force, even during initial contact between the solid and the melt. [37] Thus, the first step is to equilibrate the polymer melt or dense solution with a substrate surface after contacted, which would take a longtime and depend on the response of a bound layer to quickly remove upper unbound polymer and inspect the polymer layer before any signification characterization. [37]

O'Shaughnessy and co-workers later found that the adsorption phenomenon, which occurs at solid substrate surfaces, is irreversible. There is a powerful tendency for dense polymer layer do develop [40,41] as sticking energies per chain will increase in a portion of the number of monomer units, N, for dilute polymer solution. This effect is exploited in many technologies such as coating, lubrication, and adhesion. [42] If the monomer sticking advantage ε exceeds $k_BT$, experimental evidence showed that the relaxation times become larger that the physisorption processes were substantially irreversible. [43] In this common situation, polymer chain attach to silicon, glass or metal surface in their naturally oxidized states by hydrogen bonds ($\varepsilon \geq 4k_BT$), [44] while DNA and proteins [45] absorbed permanently on a variety materials. There are two cases of irreversible adsorption: physisorption and chemisorption. Both chemisorption and physisorption processes fill the surface with completely collapsed chains. Polymers physisorption so strongly onto solids substrate that the attached chain often seems irreversible. [42] Here is an example of chemisorption [46,47]which covalent surface-polymer bonds develop irreversibly as in applications such as polymer-fiber welding in fiber-reinforced thermoplastics and colloid stabilization by chemical grafting of polymers. [42] In general,

polymer application prefer stronger and endure interface irreversible effect than the exception.

O'Shaughnessy et al. also found that "early arriving chains had much higher fractions of bound monomers, f, than late arrivers" [48], and these f values were frozen in throughout the experiment's duration of several hours. [48] When the monomer attached to the surface, the bond never breaks became irreversible.

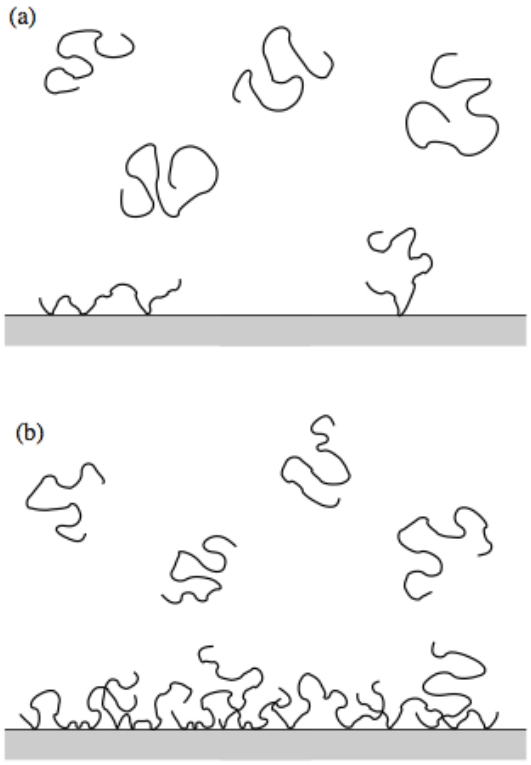


Fig.1 Two steps of polymer chain attached on substrate surface (Ref. 48)

There are two steps of forming the irreversible adsorption layer, due either to chemical bonding or strong physical interactions. (a) Early stages of layer formation. [48] The surface is almost empty and the first polymer chains to arrive attached or absorbed on the surface without interference from others. (b) After longer times, a polymer dense layer of strongly interacting chains developed on the surface become much higher than those in the bulk. [48]

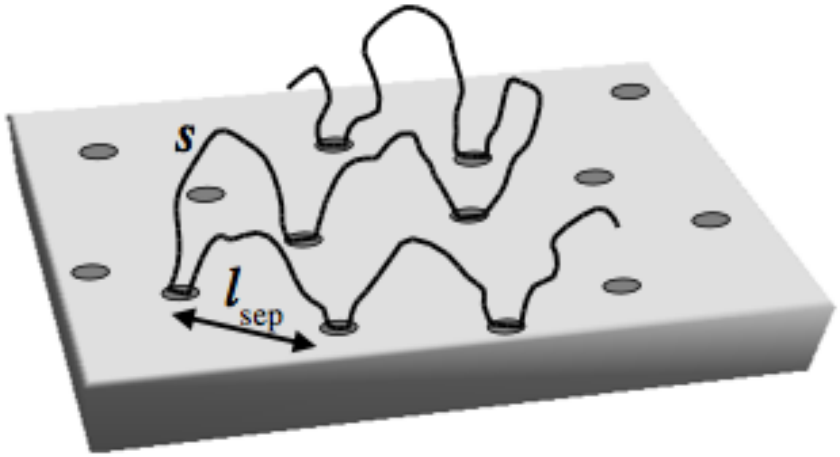


Fig.2 Typical configuration of adsorbed chain at late stages of adsorption. (Ref.48)

The late-coming chains can adsorb only onto free empty sites (shown as gray discs in Fig. 2), which are separated by $l_{sep}$. They thus form loops of s monomers, with $as^{3/5} = l_{sep}$. [48]

The late-coming chains, when adsorbing on an empty site large enough, will form bridges to nearby empty sites, which are loops of s monomers. "In order for late-coming chains to adsorb onto these surface spots, they have to form loops joining up these sites. They simulate the adsorption of chains at these late stages by assuming that the size s of such loops is the equilibrium subcoil size corresponding to $l_{sep}$." [48]

Fig. 3 Sketch of predicted final layer structure resulting from irreversible polymer adsorption. (Ref. 48)

As shown in Fig. 3, they proposed that the adsorbed layer consists of two parts (one chain

from each part is highlighted): (i) an inner region of flattened down chains making ωN contacts per chain, where ω is of order unity. (ii) A diffuse outer layer builds up from chains each making $f_N \ll N$ contacts with the surface. The values of f follow a distribution $P(f) \sim f^{-4/5}$. Each f value corresponds to a characteristic loop size for a given chain, $s \approx n_{cont}/f$. [48]

Up to now, the structures of the adsorbed polymer layer are have not been characterized in detail. This is due to the lack of experimental tools to identify such nanoscale local structures. In this work, we aim to characterize the architectures formed in the adsorbed layers from the melt onto smooth, flat solids under well-controlled contacting conditions by using x-ray reflectivity technique. The results clearly show that the formation of the flattened layer and outer-diffuse layer in the adsorbed polymer layer from the melt.

## Chapter 2 Experimental part

### 2.1 Experimental Materials

Table. 1 Basic polymer information

| Name code | Polymer | Mw | Mw/Mn | End-group |
|---|---|---|---|---|
| 100K PB | Polybutadine (1,4-addition) | 107,500 | 1.08 | / |
| 10K PB-OH | Hydroxyl polydutadine | 10,400 | 1.08 | -OH |

For 100K PB, the sample number is: P1420-Bd; while the 10K PB-OH, hydroxyl terminated polybutadine, the sample number is: P4233-BdOH, were purchased from Scientific Polymer Products and used without further purification.

### 2.2 Experimental Procedure

#### 2.2.1 Sample preparation

We produce the PB/toluene solution with 0.5%wt of PB at the normal room temperature for both 100K PB and10K PB-OH. Silicon wafers were cleaved into 1 inch×1 inch squares, used as the substrate, and were boiled in the mixture of $NH_4OH/H_2O_2/H_2O$ (1:1:3 in volume) solution for 15 minutes; then, the wafers were boiled in $H_2SO_4$/ $H_2O_2/H_2O$ (1:1:3 in volume) solution for 20 minutes and etched in $HF/H_2O$ (1:10 in volume) solution for 30s, finally the wafers over rinse and dry before use as the substrate. This procedure removes the native oxide layer and leaves the silicon surface terminated with Si-H groups.

This method produced the hydrophobic silicon substrates with an extremely thin (approximately 20Å) oxide layer on top. For 10K PB-OH, we cleaned the wafer with the same procedure as above but without HF etching to make the hydrophobic silicon surface.

The films were spun cast by photo-resist spinner (Headway Research Inc., 1-PM107D-R485) with the spinning speed at 2500 rpm for 30s to fabricate the polymer thin films. Film thickness was measured with a three-wavelength AutoEL-II ellipsometer (Rudolf

Research).

The annealing time and temperature is the key for making an absorbed layer, and not every polymer can apply on the same condition. We tried to make two different conditions to prepare the final absorbed layer. Films were annealed in the vacuum oven (10 mTorr) with 80°C and 150°C respectively. The films were annealed at 80°C, which last for 72 hours; while the films annealed at150°C, were kept under vacuum for 10 hours.

The spin-cast film is dried solvent quickly and then annealed for a longer time at melt conditions to relax the structure at the solid-melt interface. Because the spin- cast films are relatively thick, the adsorbed layer at the interface relaxes in contact with a large reservoir of unattached chains**.**

After annealing in oven for enough time, we dissolved the sample in toluene and heated in 60°C, rinse followed by every 2 hours until the thickness would not change again, as schematically shown in fig. 4.

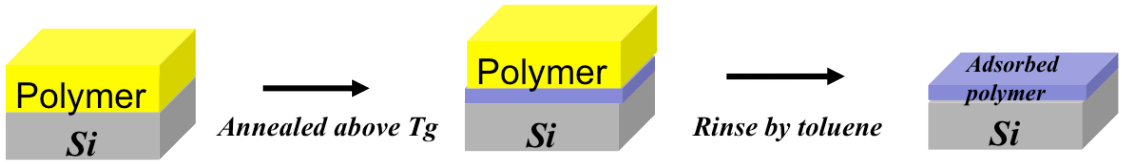


Fig. 4 Preparation of the adsorbed layer

**2.2.2 X-ray reflectivity characterization**

The x-ray reflectivity was conducted at the X10B beamline of the National Synchrotron Light Source (NSLS), Brookhaven National Laboratory (BNL), using photon energy of 14 keV, i.e. an X-ray wavelength (λ) of 0.87Å. The acquisition time was about 1 h, with the dwell time for each angle adjusted, depending on the scattering angle. The angular resolution $\Delta\theta$= 0.02°/ 0.3 mrad, and the wavelength spread, $\Delta\lambda/\lambda$, was about 0.03%, so the instrument resolution, $\Delta q_z$, is ~0.04 $nm^{-1}$, where $q_z$ is the scattering vector normal to the surface ($q_z=4\pi\sin(\theta/2)/\lambda$, θ is the scattering angle). A four-layer model, i.e. a silicon substrate, a native oxide, a polymer layer and a metal layer, was used to fit the XR data for all the polymer/metal films. [49]

Fig. 5 X10 B beamline XRR facility

### 2.2.3 Supercritical carbon dioxide ($scCO_2$) experiments

The entire samples were put into a $CO_2$ chamber shown in fig. 6.

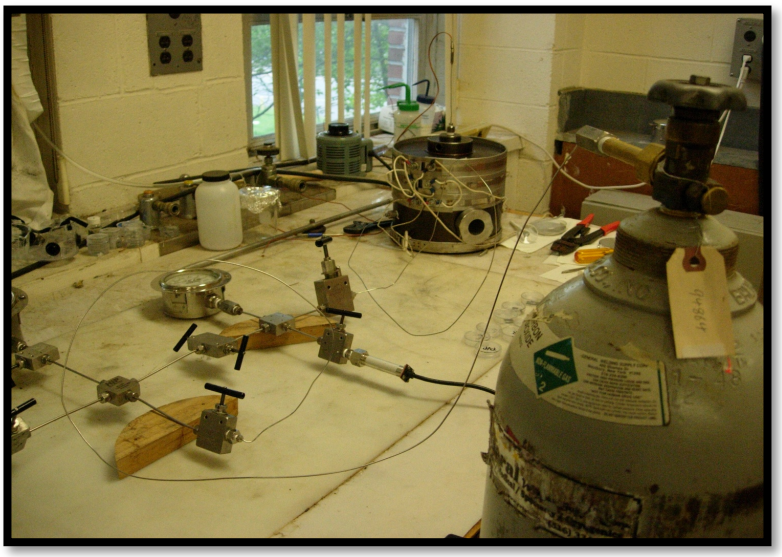

Fig. 6 $scCO_2$ chamber and other facilities

The experiment operated at a "density fluctuation ridge" condition, which the temperature T=36.6°C and the pressure is 1200psi for 3h, the films swollen in $scCO_2$. In order to preserve the swollen structure, the films were quickly depressurized to atmospheric pressure at constant temperature, typically within 10s.

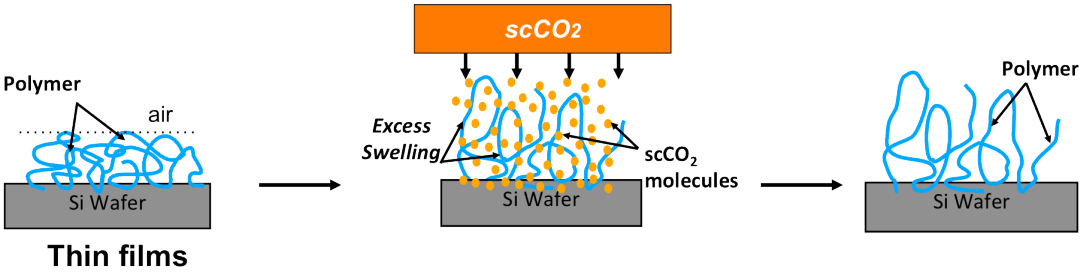


Fig. 7 $scCO_2$ experiment procedure

## Chapter 3 Results and Discussion

### 3.1 Preparation of PB adsorption layers

To characterize the absorbed layer, the first step is to make a final adsorbed layer. We tried to anneal the sample at 80°C and at150°C and found the thickness of absorbed layer increase with anneal time. Table. 1 and Figure. 8 show that 72 h and 10 h were sufficient to form a final adsorbed layer at 80°C and 150°C, respectively. The final thickness was determined to be 30Å, by using X-ray reflectivity. Note that in the case of sample without annealing, the absorbed layer was only 16Å. This imply that the adsorption process is slow to fill empty spaces at the wafer.

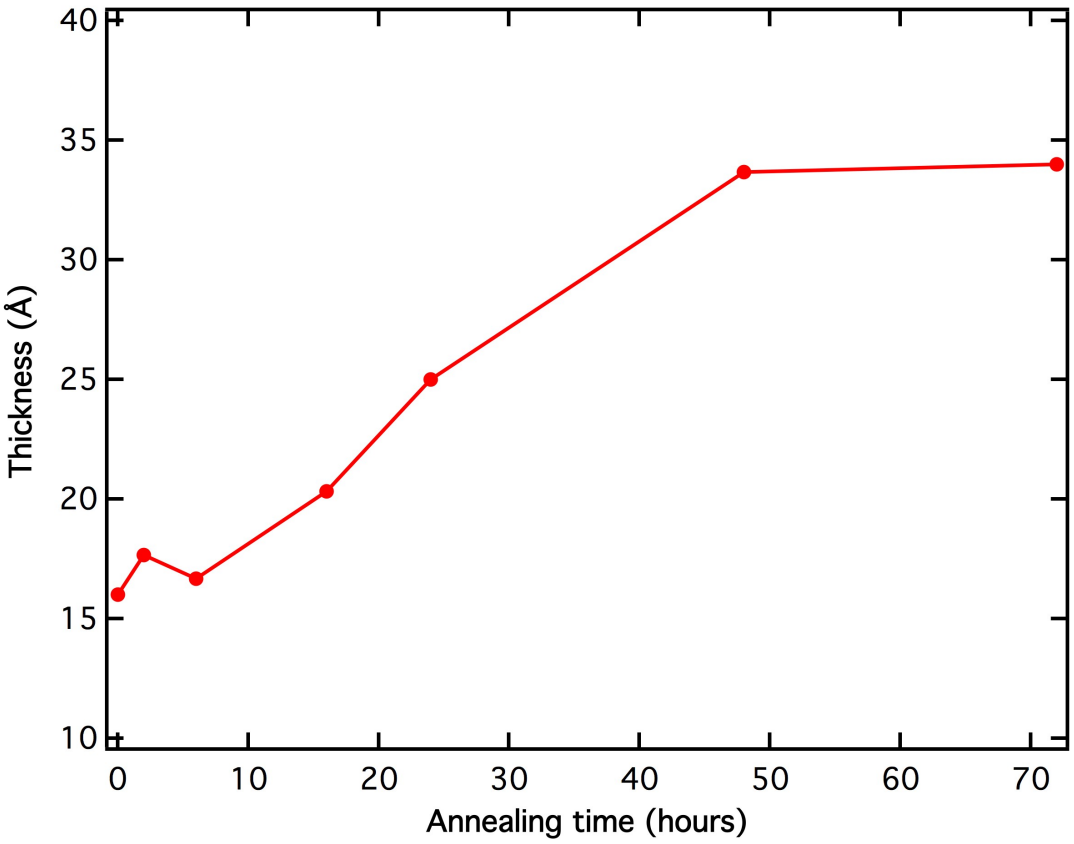


Fig. 8 Time dependence of PB adsorption layer at 80°C

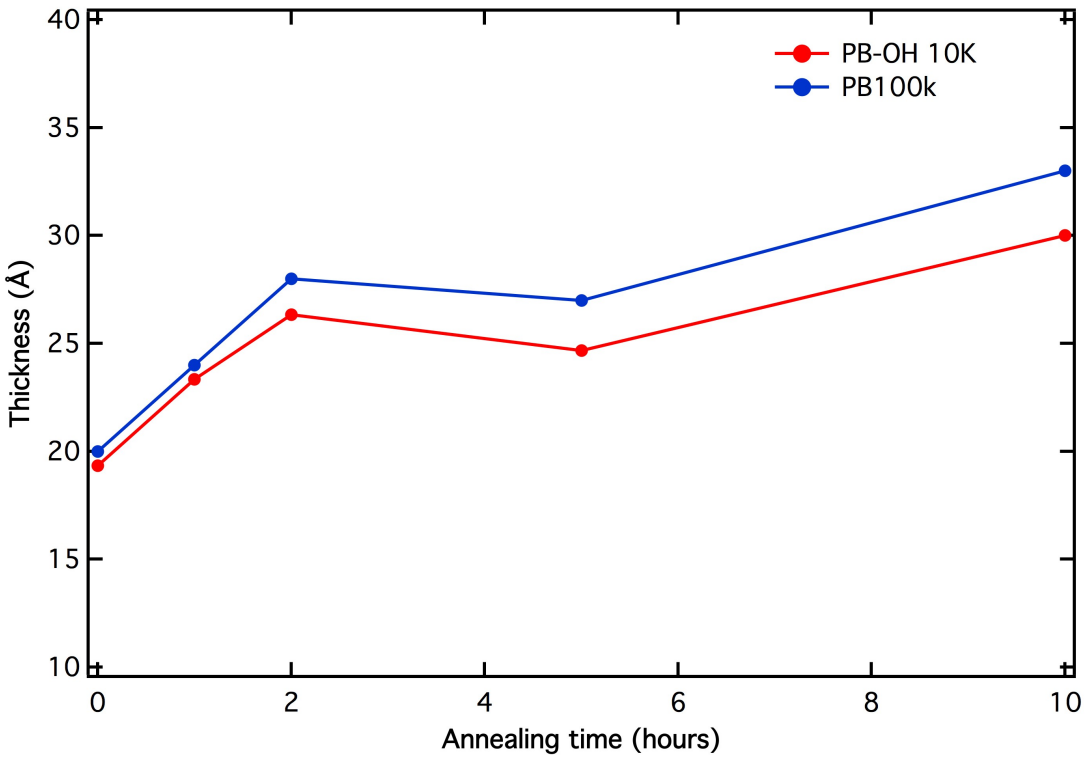


Fig. 9 Time dependence of PB adsorption layer at 150°C

We can see from fig. 8 that the thickness of the adsorbed layer increases with increasing the annealing time. Meanwhile, when the annealing temperature is 150°C, we can see from fig.9 that the thickness of the absorbed layer reached the final thickness (~30Å) within 10 hours. Thus, we assume that PB can form a final absorbed layer on the condition of 150°C within 10 hours. For lower annealing temperatures and higher molecular weights, the adsorption kinetics slows down because of the less efficient transport of chains towards the interface. [50]

### 3.2 X-ray reflectivity characterization at room temperature

For typical x-ray wavelengths, the real part of the refractive index is slightly smaller than one, which leads to the phenomenon of total external reflection. The x-rays are reflected strongly from the surface of either a crystalline or an amorphous material if the x-rays beam meets the surface at a glancing angle of a few miliradians, close to the critical angle.

The reflection of x-rays at grazing incidence has frequently been used for structure

studies of crystalline and amorphous layers and multilayers. X-ray specular reflectivity is known to give direct information on film thickness, and mean surface and interfaces roughness, whereas x-ray diffuse scattering provides information about the lateral structure of surface and interfaces. [51]

To determine thickness and roughness with high accuracy, it is essential to precisely align a sample position to the X-ray beam. The sample is mounted on a vertical sample stage, which is installed on a higher resolution goniometer. By repeatedly adjusting z and ω (or θ) positions, an optimum position is obtained in which the sample is located at the center of the X-ray beam and only half X-ray beam is detected by the detector. Then, by setting the detector (2θ) at an appropriate position, the total external reflection adjustment starts. [51]

Figure. 12 shows the data for the 100K PB sample (with HF etching) at 30°C. The data was fitted using 3-layer model, i.e. a silicon substrate, a native oxide, a polymer layer.

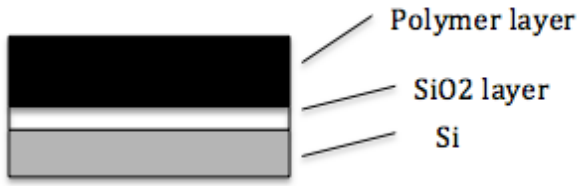


Fig. 10 Picture of a 3-layer model

The circles correspond to the observed data, while the line is the best-fit data based on 3-layer model. It is obvious that the fitting data is in good agreement with the observed data, indicating the thickness, roughness, and the dispersion value of the index of refraction of the polymer are reliable. Based on the fitting result, the dispersion was found to be $1.5\times10^{-6}$, which is much larger than that of the bulk ($\delta_{bulk}$=1.135). Since the dispersion value is the proportional to the density, the results prove that the density of the adsorbed layer increased by 50%. The total thickness is 38.8Å, which is much smaller than that of PS (Mw=100K) adsorbed layer (70Å) prepared by the same protocol.

This difference can be explained as follows: according to Gin and co-workers, the PS adsorbed layers are composed of two layers: one is high-density flatten layer and the other is a top outer diffuse layer. Since the interaction energy between PB and Si is weak enough, the toluene leaching alone is possible to remove the top diffuse outer layer.

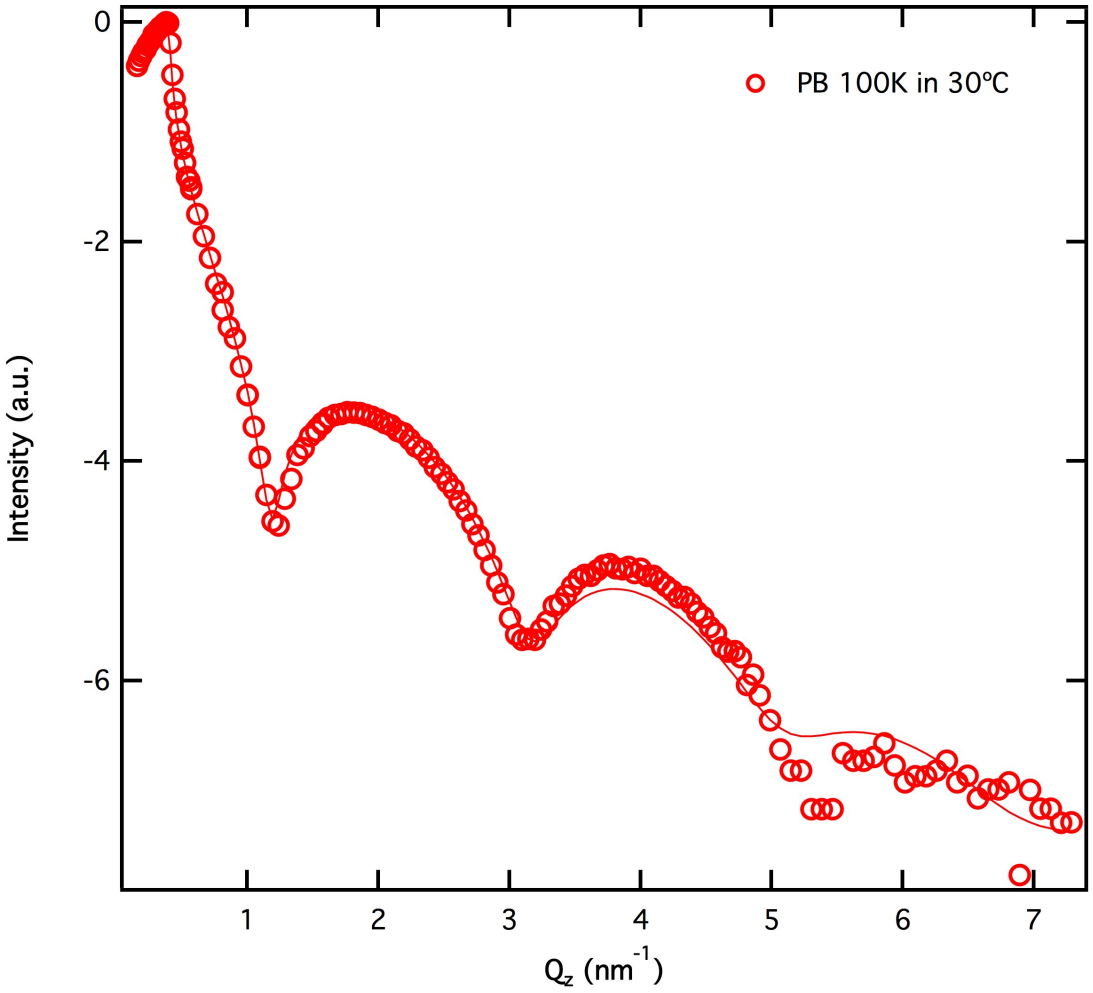


Fig. 11 XRR of PB 100K at 30°C

### 3.3 scCO$_2$ cycle experiments

To prove our hypothesis, we tried scCO$_2$ experiments. ScCO$_2$ has long been known to be a 'green' medium for polymer chemistry or material science. [49] A wide variety of polymer thin films can swell as much as 30% – 60% when exposed to scCO$_2$ within a narrow temperature and pressure regime, known as the 'density fluctuation ridge' that defines the maximum density fluctuation amplitude in CO$_2$. [49]

### 3.3.1 $scCO_2$ leaching process

In order to find out whether the absorbed layer of PB is the flatten layer, we used $scCO_2$ as a screening solvent to prove the hypothesis. Fig.16 and table.3 summarized that the thickness of the change by each process.

Table. 2 Thickness change during the toluene and $scCO_2$ leaching process.

| | | 1st cycle | | | 2nd cycle | | | 3rd cycle | | |
|---|---|---|---|---|---|---|---|---|---|---|
| | Initial thickness | $scCO_2$ | Rinse | Anneal 10h 85°C | $scCO_2$ | Rinse | Anneal 10h 85°C | $scCO_2$ | Rinse | Anneal 10h 85°C |
| 10K PB-OH w/o HF | 32Å | 37Å | 27Å | 31Å | 38Å | 24Å | 33Å | 45Å | 31Å | 34Å |
| 100K PB HF | 32Å | 48Å | 28Å | 28Å | 40Å | 28Å | 38Å | 49Å | 35Å | 38Å |
| 100K PB HF | 32Å | 50Å | 29Å | 33Å | 43Å | 30Å | 35Å | 54Å | 33Å | 36Å |

We can see from table 5 that after $scCO_2$, the PB absorbed layer was swollen, and the swelling ratios $S_f = (L - L_0)/L_0$, where $L_0$ is the original thickness of PB film and L is swollen thickness, are over 50% for PB prepared on HF etched Si substrate. The swelling ratio is consistent with spun cast PB thin film (with 25nm thick film) on silicon substrates. After the $scCO_2$ procedure, the film was rinsed immediately by toluene for 2 hours. We found the thickness after the toluene and $CO_2$ process is in good agreement with the original thickness of the adsorbed layer. We can see the thickness remains unchanged even after the second and third united washing process. Hence, we conclude that the toluene washing alone is sufficient to create the final flatten layer.

### 3.3.2 Swelling behavior of the adsorption layers

Table. 3 shows the swelling ratio of 100K PB and 10K PB-OH treated by different

conditions.

Table. 3 Swelling ratio of different PB films after the $scCO_2$ process

| Polymers | Swelling ratio |
|---|---|
| 10K PB-OH w/o HF | 16% |
| 100K PB with HF | 50% |
| 10K PB-OH with HF | 56% |

From the table, we can see the swelling ratio for the PB adsorbed films prepared on HF etched Si substrates are almost 50%, while that for the 10K PB-OH prepared on without HF etched Si is only 16%.

Hence, the polymer strongly anchored to Si substrates and cannot expand their conformations even in a good solvent.

### 3.4 Effect of interfacial energy on PB adsorption layers

Studies on polymer behavior of polymers have demonstrated that substrate/polymer interfacial interactions are crucial for controlling chain conformation, [52] and segmental mobility, [53-55] viscoelastic properties [56] and glass transition [57-62]. In semicrystalline polymers, they also affect the degree of crystallinity [63,64], crystal growth rate [64,65,66], structural morphology [64, 67-72], and orientated crystallinity [57,73].

The difference between PB adsorbed layer and PS adsorbed layer can be explained by the difference in their interfacial interactions.

Between the liquid and solid substrates, interfacial energy can be calculated using the [74] Owens-Wendt-Kaelble [75] equation:

$$\Upsilon_{ls} = \Upsilon_s + \Upsilon_l - 2\left(\Upsilon_s^d \Upsilon_l^d\right)^{1/2} - 2(\Upsilon_s^p \Upsilon_l^p)^{1/2} \qquad \text{Eq.1}$$

Which $\Upsilon_s^d$and $\Upsilon_s^p$are the dispersion and polar parts of the surface energy of the solid,

while $\Upsilon_l^d$ and $\Upsilon_l^p$ are the dispersion and polar parts of the surface energy of the liquid phase.

For $SiO_2$, $\Upsilon_s^d$ and $\Upsilon_s^p$ are 44 mJ/m$^2$ and 22 mJ/m$^2$, respectively, for PB, $\Upsilon_l^d$ and $\Upsilon_l^p$ are 48.6 mJ/m$^2$ and 0, respectively. Compare with PS, we can get $\Upsilon_l^d$ and $\Upsilon_l^p$ is 34.5 mJ/m$^2$ and 6.1 mJ/m$^2$, respectively. Using equation 1 to calculate the interfacial energy, we obtained $\Upsilon_{PB-SiO2}$= 22.1 mJ/m$^2$, and $\Upsilon_{PS-SiO2}$=5.6 mJ/m$^2$, indicating the $SiO_2$ has the stronger attraction to PS than PB. It can explain why the polymer chains are stickier to the substrate such that we need additional $CO_2$ to remove the top diffuse layer.

### 3.5 X-ray reflectivity characterization at high temperature

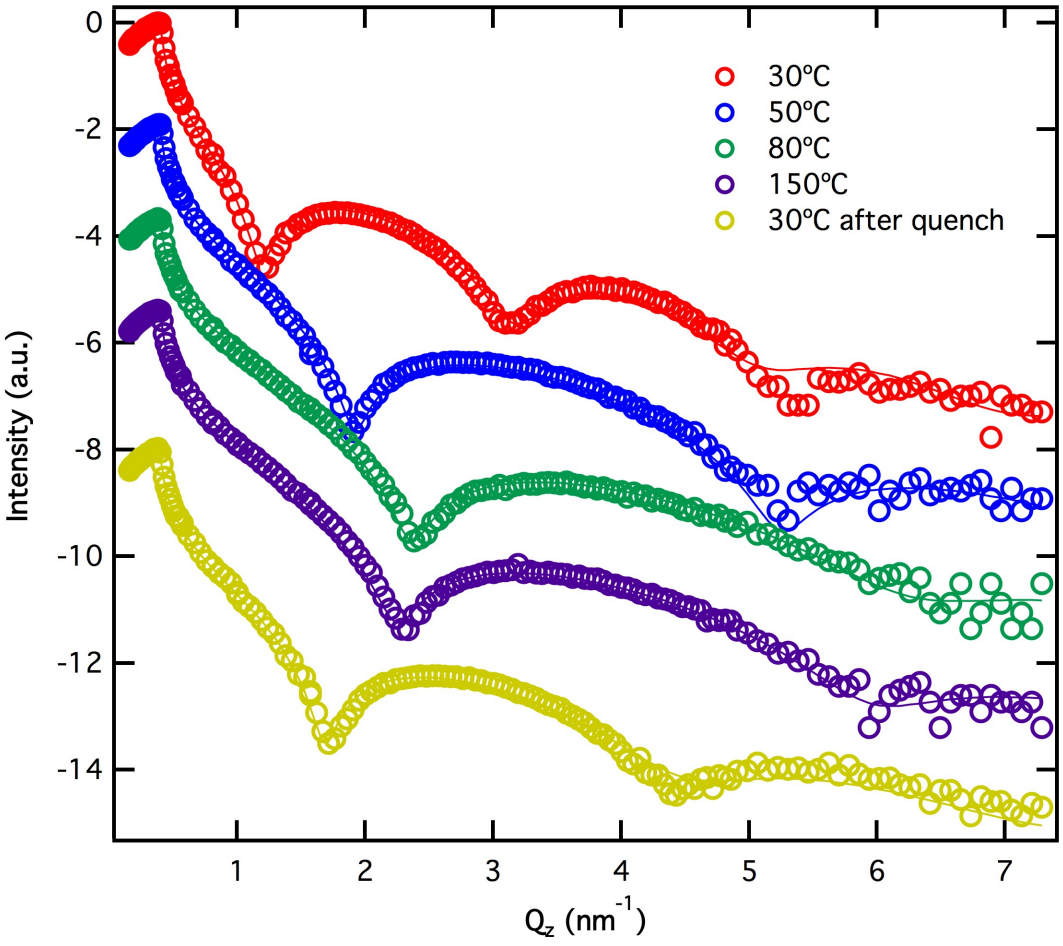


Fig. 12 100K PB XRR fitted by the 3-layer model

Fig. 13 shows the thickness change based on the temperature dependence. It is clear that the thickness decreases from 30°C to 80°C, and it becomes plateau till 150°C.

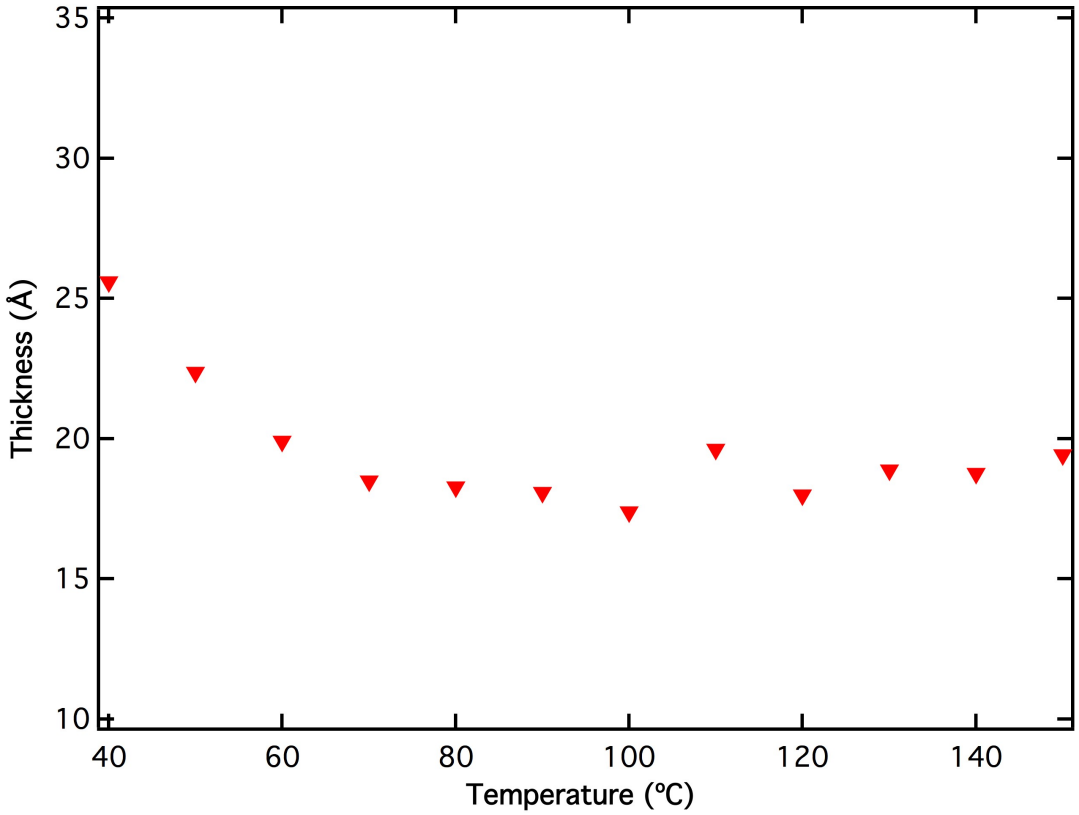


Fig. 13 Thickness of non-end functionalized PB (Mw=100K)

From 30°C to 80°C, when the polymers get the energy, they try to occupy the entire substrate as much as they can. Such that the polymer spread and the thickness decreases. When the temperature becomes higher and higher, the polymer already occupied all the area on the substrate and can not spread anymore, resulting in the constant thickness.

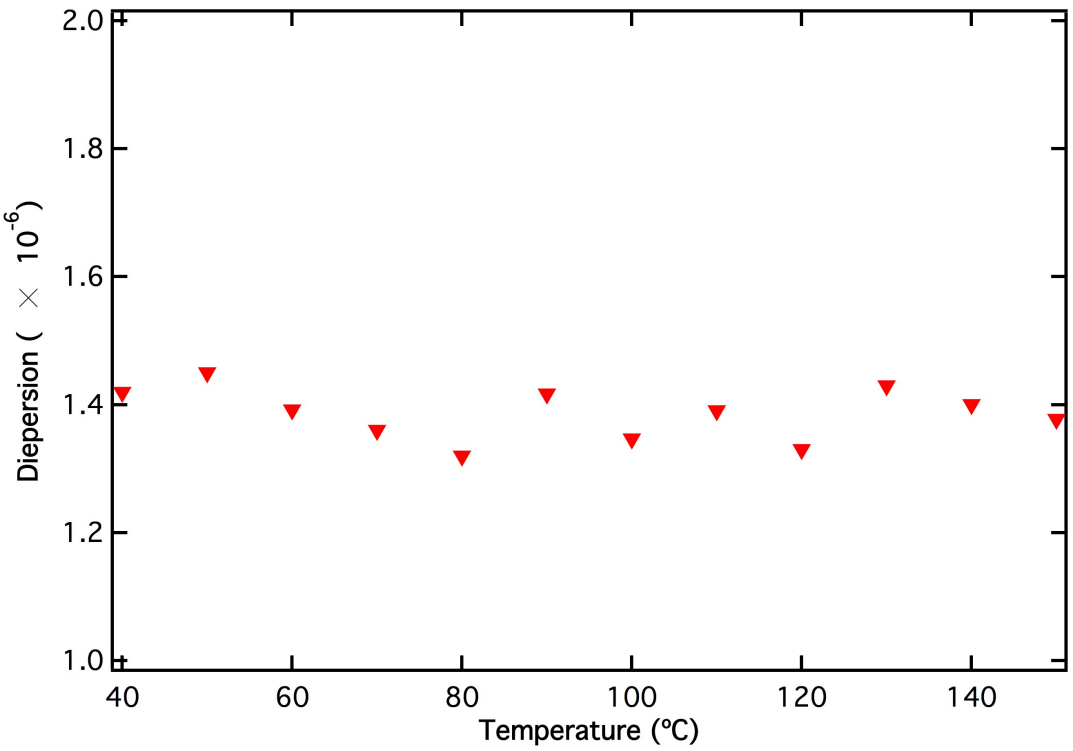


Fig. 14 Dispersion value of PB (Mw=100K)

Fig. 14 shows the temperature-dependence of the dispersion value.

From the figure.13, we can see the density remains almost constant (50% higher than the bulk) up to 150°C.

### 3.6 Discussion about Hydroxyl PB (10K PB-OH)

To see the effect of the interaction between polymer and substrate on the polymer adsorbed layer, we made the PB-OH absorbed layer in the same way as 100K PB (annealed in 150°C for 10hrs and thoroughly rinsed). The sample was tested by XRR.

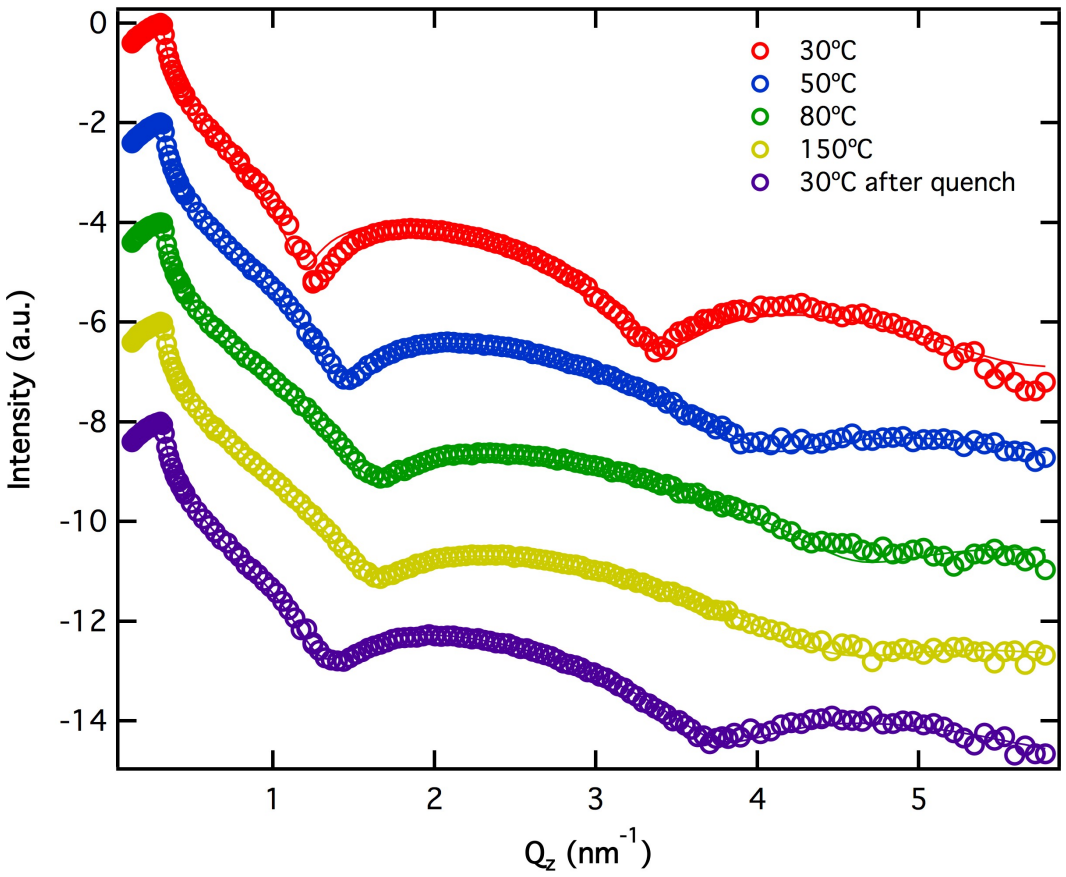


Fig. 15 XRR of PB-OH (Mw=10K) fitted by the 3-layer model

Fig. 15 showed XRR data measured from room temperature to 150°C. It is obvious that data was not fitted well in 30°C by a 3-layer model. This implies that that there is another layer within the film. To find out which model is correct, we obtained the FT profile (figure. 16).

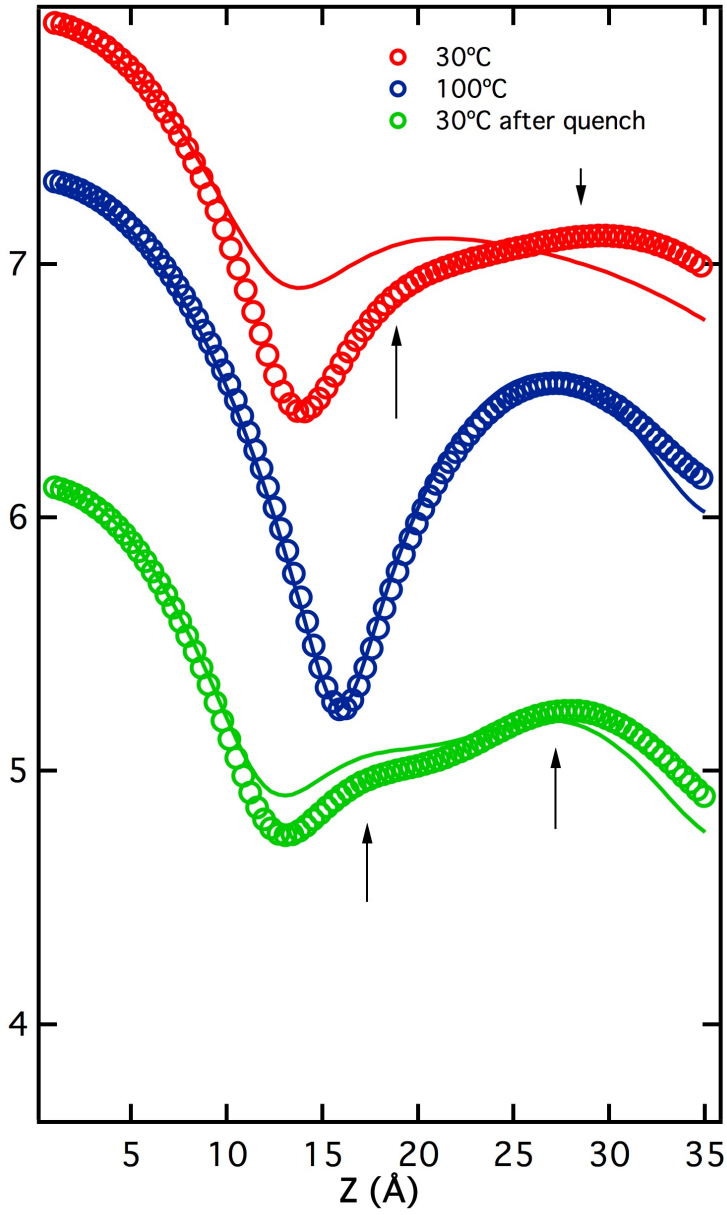


Fig. 16 Fourier transformation of 3-layer model for PB-OH (Mw=10K)

From the figure, we can see there are the main peak indicating the total thickness of the thin film, and another broad peak (indicating by the arrows). This peak indicates the presence of additional layer in the thin film. Based on the FT information, we can see clearly that the film has 2 different density layers at 30°C and it became homogenous single at 100°C. After the heating experiment, we quenched the sample to 30°C quickly and measure XRR at 30°C. As a result, we found that the film became 4 layers again.

Thus, the film is composed of two layers at 30°C as the equilibrium structure.

However, if we fit the data by four-layer model, i.e., a silicon substrate, a native oxide, a high-density polymer layer, and a low-density polymer layer.

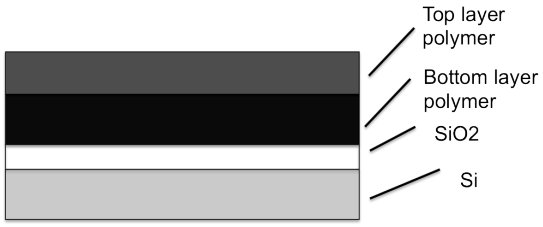


Fig. 17. 4-layer model

We can see from Fig.18 that the observed data were fitted better with a 4-layer model (Fig. 17) at 30°C than the 3-layer model.

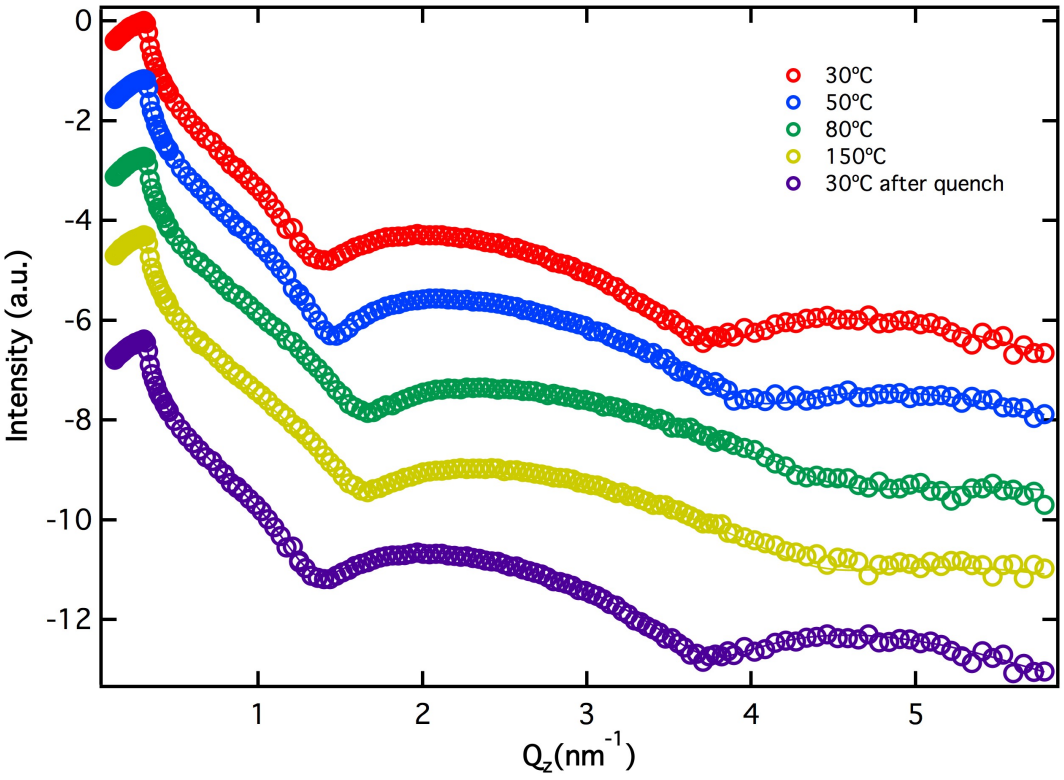


Fig. 18 XRR of non-end functionalized PB (Mw=100K) fitted by 4-layer model

At the same time, as shown in Fig. 19, the FT image of 4-layers model fitted better than

3-layers model.

From the fit image, the adsorbed layer for 10K PB-OH prepared on non-HF etched Si substrate are composed of 6.5 Å in top layer and 18.9 Å in bottom layer. The density of each layer is 1.07 $\times 10^{-6}$ and $1.41 \times 10^{-6}$, respectively.

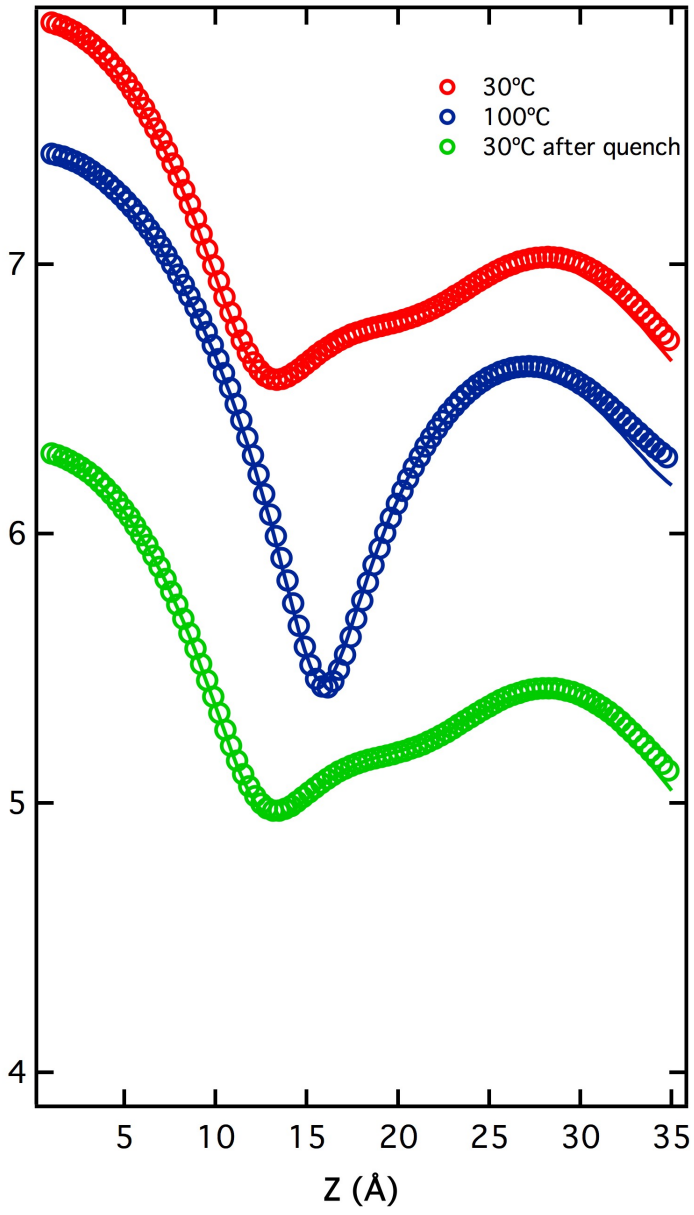


Fig. 19 FT of 4-layer model for hydroxyl PB

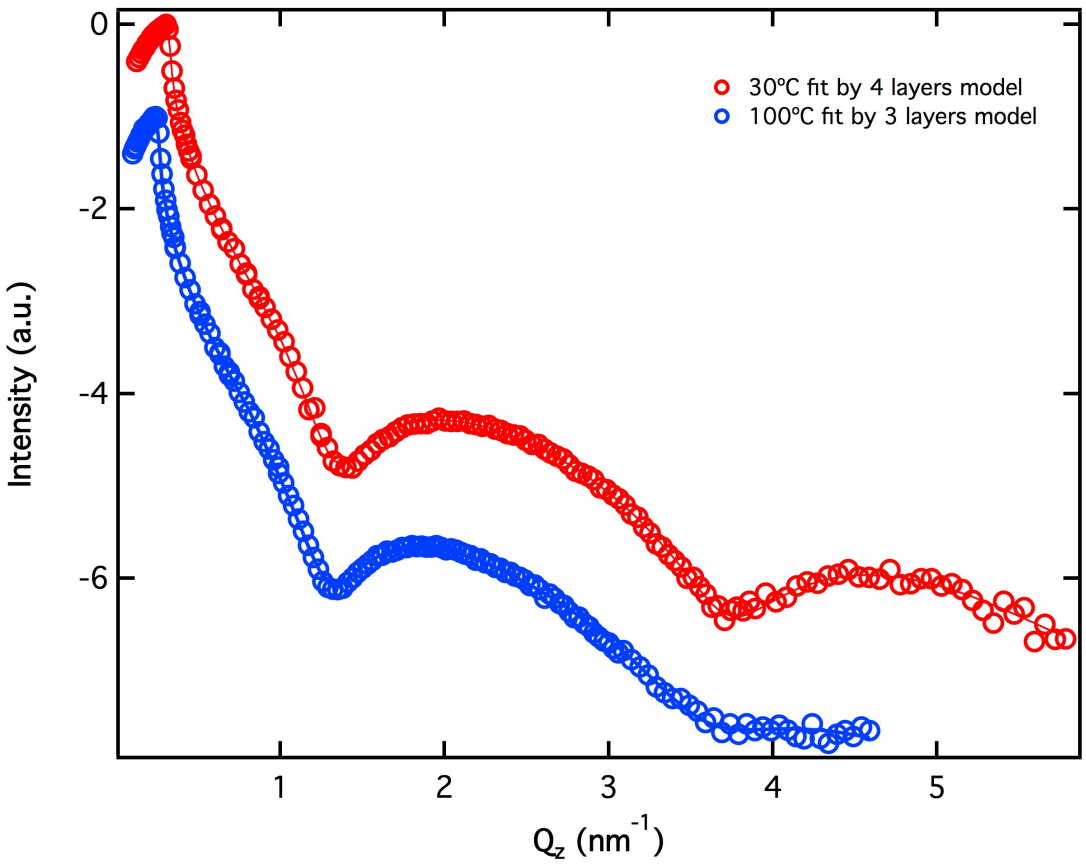


Fig. 20 30°C and 100°C 10K PB-OH fitted by 4 layers model and 3 layers model

In this case, the polymer has the –OH group, and the wafer were not etched by HF, such that polymer has stronger interaction with the wafer. Even in the high temperature, polymer still can stay on the wafer and with no thickness change. We noticed that the thickness of 100K PB going slightly up, however, after analysis by statistical method, we believed that the data is reliable. Therefore, for both 100K PB and 10K PB-OH, the thickness decreased first and did not change in the high temperature, see Fig. 22. For 10K PB-OH, which has strong interaction between polymer and silicon wafer, they form a stable adsorbed layer before increasing temperature. When increase the temperature, polymer get more energy to occupy and spread on the wafer, so that we can see the polymer become thinner and dispersion value increased from 30°C to 80°C. When it reached to 80°C, polymer already form the flatten layer such that we can see the thickness and dispersion do not change any more.

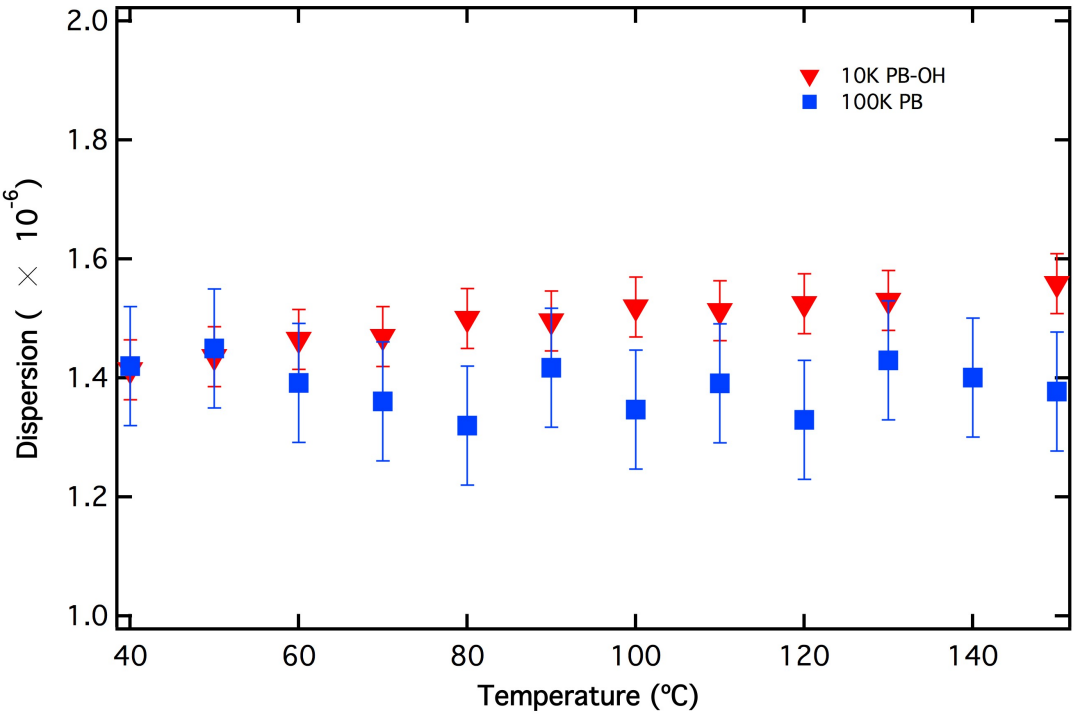


Fig. 21 Dispersion value change of 10K PB-OH and 100K PB with 3-layer model

By comparing dispersion value and thickness between 100K PB and 10K PB-OH, see Fig. 21 and Fig. 22, we can see that even they have different molecular weights and different terminated group, the dispersion value and thickness of flatten layer are almost same.

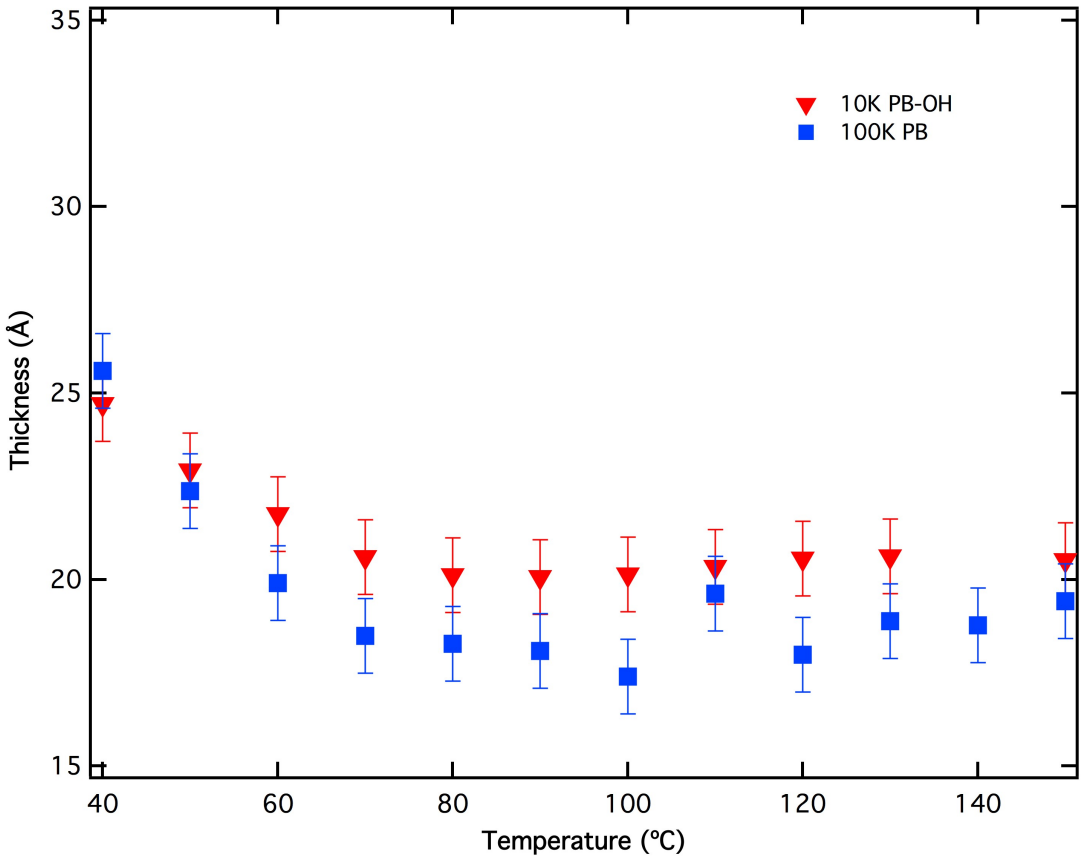


Fig. 22 Thickness change of 10K PB-OH and 100K PB with 3-layer model

## Chapter 4 Conclusions

By using X-ray reflectivity, we characterized the adsorbed PB layers from the melt onto Si substrates. As a result, we found that

I. The PB (Mw=100K) adsorbed layer is a single layer, with 30Å in thickness. The density is 40% higher than the bulk at room temperature. This is in contrast to the PS adsorbed layer which are composed of two different density layers: high-density flatten layer and low-density outer diffuse layer. Since PB/Si has weaker interfacial energy than PS/Si, toluene-leaching process alone is sufficient to reveal the high-density layer.

II. During high-temperature experiments, we found the unique behavior of the thickness and dispersion values for both 100K PB and 10K PB-OH. The thickness decreased continuously from 30°C to 80°C and became plateau (~18Å) up to 150°C, while the dispersion values remained almost constant ($\sim 1.4\times10^{-6}$) which is almost 30% higher the bulk value. Therefore, we conclude that the thickness and density of the final flattened layer does not depend on the molecular weights of the polymers and the interactions between the polymer and substrates.

## References

[1] M.M. Despotopoulou , C.W. Frank , W.D. Hinsberg , R.D. Miller , R.F.W. Pease and J.F. Rabolt Science. 273.5277 (Aug. 16, 1996): p912.

[2] Simone Napolitano, Michael Wübbenhorst. *Nature Communications 2*,Article number: 260, 1-7, (2011)

[3] Manish K. Mundra, Christopher J. Ellison, Ross E. Behling, John M. Torkelson, *Polymer* Volume 47, Issue 22, 18 October 2006, Pages 7747–7759

[4] Reiter G, Castelein G, Sommer JU, Rottele A, Thurn-Albrecht T. Phys Rev Lett 2001; 87:226101.

[5] Loo LY, Register RA, Ryan AJ. Phys Rev Lett 2000; 84: 4120-3.

[6] Jones BA, Torkelson JM. J Polym Sci Part B Polym Phys 2004; 42: 3470-5.

[7] Kim SD, Torkelson JM. Macromolecules 2002; 35:5943-52.

[8] Orts WJ, van Zanten JH, Wu WL, Satija SK. Phys Rev Lett 1993; 71:867-70.

[7] Oh WT, Ree MH. Langmuir 2004; 20: 6932-9.

[9] Kanaya T, Miyazaki T, Watanabe H, Nishida K, Yamana H, Tasaki S, et al. Polymer 2003; 44:3769-73.

[10] Soles CL, Douglas JF, Jones RL,Wu WL. Macromolecules 2004;37: 2901-8.

[11] Kawana S, Jones RAL. Phys Rev E 2001; 63:021501.

[12] Beaucage G, Composto R, Stein RS. J Polym Sci Part B Polym Phys 1993; 31:319-26.

[13] Mukherjee M, Bhattacharya M, Sanyal MK, Geue T, Grenzer J, Pietsch U. Phys Rev E 2002; 66: 061801.

[14] Manish K. Mundra, Christopher J. Ellison, Ross E. Behling, John M. Torkelson, Polymer Volume 47, Issue 22, 18 October 2006, Pages 7747–7759.

[15]) Sanyal, M. K.; Basu, J. K.; Datta, A.; Banerjee, S. Europhys. Lett. 1996, 36, 265–270.

[16] Laschitsch, A.; Bouchard, C.; Habicht, J.; Schimmel, M.; Ruhe, J.; Johannsmann, D. Macromolecules 1999, 32, 1244–1251.

[17] Doumenc, F.; Guerrier, B.; Allain, C. Europhys. Lett. 2006,76, 630–636.

[18] Tsui, O. K. C.; Wang, Y. J.; Lee, F. K.; Lam, C.-H.; Yang, Z. Macromolecules 2008, 41, 1465–1468.

[19] Baschnagel, J.; Varnik, F. J. Phys.: Cond. Matt. 2005, 17, R851–R953.

[20] Keddie, J. L.; Jones, R. A. L.; Cory, R. A. Faraday Diss. 1994, 98, 219–230.

[21] Tsui, O. K. C.; Zhang, H. F. Macromolecules 2001, 34, 9139–9142.

[22] Forrest, J. A.; Dalnoki-Veress, K. Adv. Colloid Interface Sci. 2001, 94, 167–196.

[23] Herminghaus, S.; Jacobs, K.; Seemann, R. Eur. Phys. J. E 2001, 5, 531–538.

[24] Ellison, C. J.; Torkelson, M. Nat. Mater. 2003, 2, 695–670.

[25] Tsui, O. K. C., Polymer Thin Films; World Scientific: Hackensack, NJ, 2008; Chapter 11, pp 267-294.

[26] Physics of Polymer Surfaces and Interfaces; Sanchez, I. C., Ed.; Butterworth-Heinemann: Boston, 1992.

[27] Liquids at Znterfaces,Proceedings of the Les Houches Summer School Session X L VZZe Charvolin, J., Joanny, J.-F., Zinn-Justin, J., Eds.; Elsevier: Amsterdam, 1989.

[28] Kumar, S. K.; Vacatello, M.; Yoon, D.Y. J. Chem. Phys. 1988, 89, 5206.

[29] Ten Brinke, G.; Ausserr, D.; Hadziioannou, G. J. Chem. Phys. 1988,89, 4374.

[30] Mansfield, K.;Theodorou,D. N.Macromolecules 1989,22,3143.

[31] Yethiraj, A.; Hall, C. K. Macromolecules 1990,23, 1865.

[32] Bitsanis, I.; Hadziioannou, G. J. Chem. Phys. 1990, 92, 3827.

[33] Smith, G. D.; Yoon, D. Y.; Jaffe, R. L. Macromolecules 1992, 25, 7011

[34] Gunter Reiter, Macromolecules (1994) Volume: 27, Issue: 11, Publisher: American Chemical Society; 3046-3052

[35] Tsui, O. K. C., Polymer Thin Films; World Scientific: Hackensack, NJ, 2008; Chapter 11, 267-294.

[36] Akira Takahashi, Masami Kawaguchi, Hideyuki Hirota, and Tadaya Kato, *Macromolecules* 1980,13,884-889

[37] Guiselin, O. Europhys. Lett. 1992, 17, 225.

[38] By brushlike,we mean that lateral repulsive interactions are an important feature when the layer is swollen with good solvent. The result is a strong dependence of the swollen layer's height, $h_{swollen}$, on molecular weight, approaching $h_{swollen} \sim N$.

[39] Alexander, S. J. Physics (Paris) 1977, 38, 983.

[40] G. J. Fleer, M. A. Cohen Stuart, J. M. H. M. Scheutjens, T. Cosgrove, and B. Vincent, *Polymers at Interfaces* (Chapman and Hall, London, 1993).

[41] P. G. de Gennes, Macromolecules **14,** 1637 (1981); 15, 492 (1982);A. N. Semenov and J.-F. Joanny, Europhys. Lett. **29,** 279 (1995); M. Aubouy, O. Guiselin, and E. Raphael, Macromolecules **29,** 7261 (1996).

[42] Ben O'Shaughnessy1 and Dimitrios Vavylonis, Physics Review Letters, 2003,

volume 90, number 5

[43] H. M. Schneider, P. Frantz, and S. Granick, Langmuir 12, 994 (1996); J. F. Douglas et al., J. Phys. Condens. Matter 9, 7699 (1997).

[44] M. D. Joesten and L. J. Schaad, Hydrogen Bonding (Dekker, New York, 1974).

[45] V. Hlady and J. Buijs, Curr. Opin. Biotechnol. 7,72 (1996); P.O. Brown and D. Botstein, Nat. Genet. Suppl. 21, 33 (1999).

[46] T. J. Lenk, V. M. Hallmark, and J. F. Rabolt, Macromolecules 26, 1230 (1993); K. Konstadinidis et al., Langmuir 8, 1307 (1992).

[47] J. S. Shaffer and A. K. Chakraborty, Macromolecules 26, 1120 (1993).

[48] Ben O'Shaughnessy and Dimitrios Vavylonis, The European Physical Journal E: Soft matter and Biological Physics, Volume 11, Number 3 (2003).

[49] Tadanori Koga et al. Polymer film metallizationJ. Appl. Cryst. (2007). 40, 684–686.

[50] Simone Napolitano, Michael Wübbenhorst, Nature Communications2,Article number: 260

[51] Isao Kojima, Boquan LI, *The Rigaku Journal* Vol. 16, number 2, 199

[52] Kraus J, Muller-Buschbaum P, Kuhlmann T, Schubert DW, Stamm M. Confinement effects on the chain conformation in thin polymer films. Europhys Lett 2000;49(2):210–6.

[53] Zheng X, Sauer BB, Vanalsten JG, Schwartz SA, Rafailovich MH, Sokolov J, Rubinstein M. Reptation dynamics of a polymer melt near an attractive solid interface. Phys Rev Lett 1995;74(3):407–10.

[54] Zheng X, Rafailovich MH, Sokolov J, Strzhemechny S, Schwarz SA, Sauer BB, Rubinstein M. Long-range effects on polymer diffusion induced by a bounding interface. Phys Rev Lett 1997;79(2):241–4.

[55] Lin EK, Wu WL, Satija SK. Polymer interdiffusion near an attractive solid substrate. Macromolecules 1997;30(23):7224–31.

[56] Hu HW, Granick S. Viscoelastic dynamics of confined polymer melts. Science 1992;258(5086):1339–42.

[57] Keddie JL, Jones RAL, Cory RA. Size-dependent depression of the glass transition temperature in polymer films. Europhys Lett 1994;27(1):59–64.

[58] Keddie JL, Jones RAL, Cory RA. Interface and surface effects on the glass-

transition temperature in thin polymer films. Faraday Dis Chem Soc

1994;98: 219–30.

[59] Forrest JA, DalnokiVeress K, Dutcher JR. Interface and chain confinement

effects on the glass transition temperature of thin polymer films. Phys Rev E

1997;56(5):5705–16.

[60] Fryer DS, Peters RD, Kim EJ, Tomaszewski JE, Pablo JJ, Nealey PF, White CC, Wu

WL. Dependence of the glass transition temperature of polymer films on interfacial energy and thickness. Macromolecules 2001; 34(16):5627–34.

[61] Fryer DS, Nealey PF, Pablo JJ. Scaling of Tg and reaction rate with film thickness in photoresist: a thermal probe study. J Vac Sci Technol B 2000; 18(6):3376–80.

[62] Pu Y, Ge SR, Rafailovich M, Sokolov J, Duan Y, Pearce E, Zaitsev V, Schwarz S. Surface transitions by shear modulation force microscopy. Langmuir 2001;17(19):5865–71.

[63] Despotopoulou MM, Frank CW, Miller RD, Rabolt JF. Kinetics of chain organization in ultrathin poly(di-n-hexylsilane) films. Macromolecules 1996;29(18):5797–804.

[64] Schönherr H, Frank CW. Ultrathin films of poly(ethylene oxides) on oxidized silicon. 1. Spectroscopic characterization of film structure and crystallization kinetics. Macromolecules 2003;36(4):1188–98.

[65] Taguchi K, Miyaji H, Izumi K, Hoshino A, Miyamoto Y, Kokawa R. Crystal growth of isotactic polystyrene in ultrathin films: film thickness dependence. J Macromol Sci B 2002;41(4–6):1033–42.

[66] Schönherr H, Frank CW. Ultrathin films of poly(ethylene oxides) on oxidized silicon 2. In situ study of crystallization and melting by hot stage AFM. Macromolecules 2003;36(4):1199–208.

[67] Mellbring O, Kihlman Øiseth S, Krozer A, Lausmaa J, Hjerberg T. Spin coating and characterization of thin high-density polyethylene films. Macromolecules 2001; 34(21):7496–503.

[68] Reiter G, Sommer JU. Polymer crystallization in quasi-two dimensions I. Experimental results. J Chem Phys 2000; 112(9):4376–83.

[69] Reiter G, Sommer JU. Polymer crystallization in quasi-two dimensions. II. Kinetic models and computer simulations. J Chem Phys 2000;112(9):4384–93.

[70] Reiter G, Sommer JU. Crystallization of adsorbed polymer monolayers. Phys Rev Lett 1998; 80(17):3771–4.

[71] Zhang F, Liu J, Huang H, Du B, He T. Branched crystal morphology of linear polyethylene crystallized in a two-dimensional diffusion-controlled growth field. Eur Phys J E 2002;8(3): 289–97.

[72] Taguchi K, Miyaji H, Izumi K, Hoshino A, Miyamotoand Y, Kokawa R. Growth shape of isotactic polystyrene crystals in thin films. Polymer 2001;42(17):7443–7.

[73] Bartczak Z, Argon AS, Cogen RE, Kowalewski T. The morphology and orientation of polyethylene in films of sub-micron thickness crystallized in contact with calcite and rubber substrates. Polymer 1999;40(9):2367–80.

[74] Avigail Hershkovits-Mezumana, Hannah Harel, Yantian Wang, Chunhua Li, Jonathan C. Sokolov, Miriam H. Rafailovich, Gad Marom, Composites Part A: Applied Science and Manufacturing, Volume 41, Issue 9, September 2010, Pages 1066–1071

[75] Kwok, D. Y.; Neumann, A. W. Adv. Colloid Interface Sci. 1999, 81, 167–249.